

INTEGRATED GEOSPATIAL AND MULTI-CRITERION ANALYSIS OF FLOOD PHYSICAL VULNERABILITY IN MOKWA LGA, NIGER STATE, NIGERIA

Karimatu Lami Abdullahi

Department of Computing and Applied Sciences, Baze University, Abuja, Nigeria

*Corresponding Author Email Address: karimatu.abdullahi@bazeuniversity.edu.ng

ABSTRACT

Flooding remains a persistent threat in Mokwa Local Government Area, Niger State, due to a combination of natural topographic conditions and human-induced land changes. The study used geospatial analysis and multi-criteria decision-making to assess flood vulnerability by integrating eleven key physical and environmental factors. Data were obtained from NiMet, SRTM, Landsat-9 imagery, and the HWSO. The Analytical Hierarchy Process (AHP) was used to assign factor weights, and the final vulnerability map was developed using weighted and fuzzy overlay techniques in ArcGIS. The resulting flood vulnerability map classified the area into five categories: Very Low (223 km²), Low (303 km²), Medium (1,473 km²), High (1,624 km²), and Very High (516 km²), out of a total of 4,139 km². This means that over 87% of the land area falls under Medium to Very High vulnerability classes. Land Use/Land Cover (0.198), Elevation (0.168), and Rainfall (0.148) were identified as the most influential factors. The study recommends restricting development in High and Very High zones, enhancing drainage in built-up areas, promoting vegetation and soil conservation in clay-rich zones, and integrating flood risk maps into local planning. The approach illustrates how spatial analysis combined with the Analytic Hierarchy Process (AHP) can support evidence-based flood mitigation and informed land use planning in flood-prone areas.

Keywords: Flood Vulnerability, Geospatial Analysis, Analytical Hierarchy Process (AHP), Fuzzy Overlay, Land Use/Land Cover (LULC) and Mokwa LGA

INTRODUCTION

Flooding remains the most frequent and destructive natural disaster globally, affecting more people annually than any other hazard (Babati et al. 2022). Driven by climate change, sea-level rise, and extreme weather events, flood disasters have increased in both frequency and severity over the past decades (Muzzamil et al. 2020). Floods account for over 44% of all-natural disasters worldwide, displacing more than 200 million people and causing billions of dollars in economic losses each year (Chumky et al. 2022). Factors such as urban expansion into flood-prone zones, deforestation, and inadequate drainage infrastructure have compounded global flood vulnerability, especially in low- and middle-income regions (Singh et al. 2023).

This growing global trend is acutely reflected across Africa, where climate variability, rapid population growth, and weak infrastructural systems intensify exposure to flooding (Isa et al. 2023). In 2022 alone, over 4 million people across 20 African countries were affected by floods, particularly in West and Central Africa (Babati et al. 2025). The consequences are widespread, including

disrupted livelihoods, destroyed infrastructure, displaced populations, and increased outbreaks of waterborne diseases (Bello et al. 2022). With urban planning often lagging behind urbanization, African cities and rural communities alike remain highly vulnerable to both flash and riverine flooding (Okorafor and Chikwue 2021). Nigeria, as Africa's most populous country, continues to grapple with increasing flood occurrences and their devastating impacts (Cirella and Iyalomhe 2018). Historical events such as the 2012 and 2022 floods left millions displaced, thousands of hectares of farmland submerged, and hundreds of lives lost (Isukuru et al. 2024). The 2022 flood alone killed over 600 people, affected more than 1.4 million citizens, and caused long-lasting socio-economic damage across multiple states (Olamilekan et al. 2024). These flood events are most intense in areas adjacent to major river systems, such as the Niger and Benue rivers, where topographic and infrastructural vulnerabilities intersect (Umar and Gray 2023).

Among the regions most affected is Niger State in North-Central Nigeria. Bordered by the River Niger and intersected by various tributaries, Niger State is consistently listed among the most flood-prone states in the country (Musa et al. 2015). Local Government Areas (LGAs) like Lavun, Gbako, and Mokwa are regularly impacted by seasonal floods that destroy homes, displace families, and disrupt transportation and agriculture (Ndanusa et al. 2022). In 2022, large areas of farmland were submerged, resulting in significant economic losses and heightened food insecurity (Akoji et al. 2025). Yet despite these repeated disasters, comprehensive vulnerability assessments at the local level remain insufficient.

Mokwa Local Government Area, in particular, stands out due to its high exposure to flood hazards. Located along the banks of the River Niger, Mokwa is characterized by low-lying terrain, poor drainage systems, high rainfall intensity during the wet season, and increasing pressure from agricultural expansion and settlement near waterways (Nagya et al. 2024). The situation escalated further in June 2025, when Mokwa experienced a devastating flood event following prolonged rainfall. The flood submerged numerous communities, displaced thousands of residents, and caused extensive damage on farmlands, road infrastructure, and public facilities (Egigogo 2025). This recent disaster stresses the urgent need for a spatially informed, data-driven vulnerability assessment to effectively guide response and preparedness strategies in the affected area.

Given the complexity and recurrence of flood events in Mokwa, there is a need for a more integrative approach to vulnerability assessment. Globally, disaster risk reduction has shifted toward the use of multi-criteria decision-making tools, such as the Analytic Hierarchy Process (AHP), which enable researchers and planners to combine multiple environmental and physical factors into a

single composite analysis (Gacu et al. 2025). Among the components of vulnerability, physical vulnerability remains especially critical in regions like Mokwa, where the terrain, soil characteristics, drainage density, and land use patterns directly influence flood severity and impact.

This study employs a multi-criteria assessment framework centered on physical vulnerability to evaluate flood risk in Mokwa. By integrating variables such as soil organic carbon, silt content, sand content, clay content, distance to built-up area, distance to road, elevation, rainfall, slope, drainage density, distance to river and land use/land cover within a GIS environment, and applying AHP to assign relative weights, the study provides a detailed, spatially explicit vulnerability map. Unlike previous studies that often rely solely on historical rainfall or flood incidence data, this research uses a layered, analytical approach that reflects the spatial heterogeneity of risk within the study area.

STUDY AREA

Mokwa Local Government Area (LGA) is situated in the southwestern part of Niger State, Nigeria. Geographically, it lies between latitudes 9°10'N and 10°00'N and longitudes 4°25'E and 5°20'E, placing it within Nigeria's central region. Relative to its surroundings, Mokwa shares boundaries with Bida LGA to the north, Katcha and Lapai LGAs to the east and northeast, Edu LGA in Kwara State to the south, and Borgu LGA (Kebbi State) to the west (Figure 1). The area serves as a strategic transport and trade corridor, linking northern and southwestern Nigeria through major federal roads and rail routes. Mokwa experiences a tropical savanna climate (Aw), characterized by distinct wet and dry seasons. The rainy season typically spans from April to October, with peak between July and September, while the dry season extends from November to March. Annual rainfall ranges from 1,000 mm to 1,300 mm, and temperatures fluctuate between 24°C and 37°C, with the hottest months occurring from February to April (Odekunle 2004). Humidity is relatively high during the wet season and low during the Harmattan period, which brings dry and dusty winds from the Sahara between December and February.

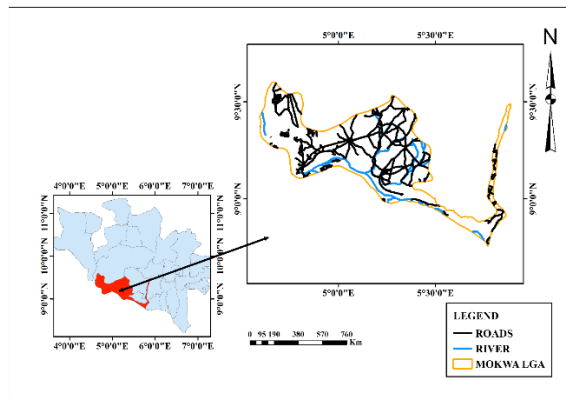


Figure 1: Index map of Niger State showing the delineation of the study area (Mokwa LGA).

Hydrologically, Mokwa is richly endowed with water resources, most notably the River Niger, which forms its southern boundary (Abrate et al. 2013). The area also features seasonal streams and tributaries that support agricultural and domestic activities. The Jebba Dam and Reservoir, located just southwest of Mokwa, play

a significant role in regional water regulation. Despite these resources, parts of Mokwa are vulnerable to seasonal flooding, particularly in the low-lying floodplains adjacent to the River Niger (Musa et al. 2015). Poor drainage infrastructure in rural communities exacerbates this vulnerability during periods of heavy rainfall. The geomorphological landscape of Mokwa consists mainly of undulating plains, floodplains, and isolated rocky outcrops (Alhaji 2022). The underlying geology of the area consists primarily of Precambrian basement complex rocks, while the floodplains are characterized by alluvial deposits. Elevations generally range from 100 to 250 meters above sea level, with gentle slopes that favor both agriculture and water accumulation (Baba et al. 2022). The soils are mostly sandy loam and alluvial, which are fertile but susceptible to erosion and flooding when vegetation cover is removed (Musa et al. 2022).

Vegetation in Mokwa is typical of the Southern Guinea Savanna, characterized by a mix of tall grasses and scattered trees such as baobab, shea, and acacia (Mustapha et al. 2022). Along riverbanks, denser gallery forests are present, supporting biodiversity and protecting river channels from erosion (Jidauna et al. 2017). However, increasing human activities, such as farming, grazing, and fuelwood harvesting, have led to significant vegetation degradation. This loss of vegetative cover has heightened the risk of surface runoff and soil erosion, contributing to the area's flood vulnerability (Baba et al. 2022).

MATERIALS AND METHODS

The methodology adopted for this study integrates multiple geospatial datasets and multi-criteria decision analysis to assess flood vulnerability using the Analytical Hierarchy Process (AHP) and fuzzy overlay techniques. The key datasets used include the 2024 annual average rainfall data obtained from the Nigerian Meteorological Agency (NiMet), topographic maps such as slope and elevation derived from the Shuttle Radar Topography Mission (SRTM) 30m resolution DEM, and hydrological layers including rainfall distribution, distance to rivers, and drainage density generated using hydrology tools in ArcGIS. Additional anthropogenic and environmental factors were considered, including the distance to built-up areas and distance to roads. These were extracted from the 2023 land use/land cover (LULC) classification of the study area, which was derived from Landsat-9 satellite imagery and classified using supervised classification in ERDAS Imagine. Soil data layers—clay, sandy, and silt maps, as well as Soil Organic Carbon (SOC) were sourced from the Harmonized World Soil Database (HWSD) and reprojected to match the coordinate reference system of the other spatial datasets.

During the data pre-processing phase, all raster layers were clipped to the study area, resampled to a common spatial resolution of 30m, and converted into thematic raster layers where necessary using ArcGIS and QGIS. Each layer was reclassified into five classes based on natural breaks (Jenks), quantiles, or expert knowledge, where class values ranged from 1 (very low vulnerability) to 5 (very high vulnerability). Proximity layers such as distance to river, road, and built-up areas were generated using the Euclidean Distance tool in ArcGIS. For flood vulnerability classification, the Analytical Hierarchy Process (AHP) was employed to assign weights to each factor based on their relative importance in contributing to flood risk. A pairwise comparison matrix was constructed, and expert judgment was applied to score the comparative influence of each factor on flooding. The

eigenvector method was used to derive the final weights, and the Consistency Ratio (CR) was computed to ensure reliability (acceptable if $CR < 0.1$). The weighted layers were then combined using the Weighted Overlay tool in ArcGIS to produce the AHP-based flood vulnerability map.

Subsequently, a fuzzy overlay analysis was performed to enhance the classification by accounting for the uncertainty and continuous nature of environmental phenomena. Each input layer was normalized using fuzzy membership functions (e.g., small, large, linear) based on their relationship to flood susceptibility. For instance, slope was assigned a 'fuzzy small' function, as lower slopes indicate higher flood risk. The Fuzzy Overlay tool with the Gamma operator ($\gamma = 0.9$) was applied to integrate all fuzzy-normalized layers, resulting in a continuous flood vulnerability surface. Finally, the output was classified into five vulnerability zones: Very Low, Low, Medium, High, and Very High, to support effective spatial planning and disaster risk management.

RESULTS AND DISCUSSION

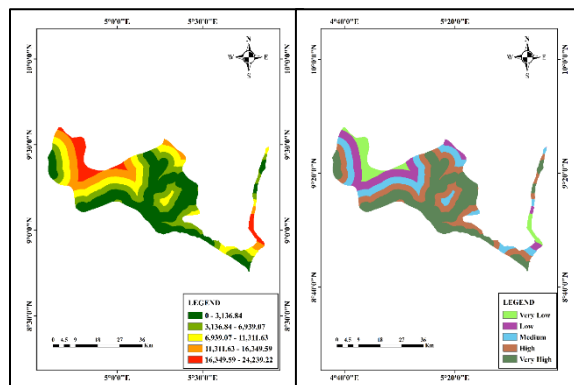


Figure 2: Distance to River

Figure 2 show the spatial distribution and reclassification of distance to rivers in relation to flood physical vulnerability in the study area. On the left side, the map shows the raw distance-to-river data, with values ranging from 0 to 24,239.22 meters. Areas closer to rivers are represented by warmer colors (red, orange, yellow), while areas farther from rivers are represented by cooler colors (green tones). On the right side, the same data has been reclassified into five distinct categories of flood vulnerability based on proximity to rivers: "Very High" vulnerability (class 5) to rivers, while "Very Low" vulnerability (class 1) rivers. Proximity to rivers is a key flood risk. Flooding due to direct overbank flow during heavy rainfall or river overflow events. The reclassified map clearly supports this concept: regions near river channels are classified as "Very High" and "High" in terms of flood vulnerability. These areas are most susceptible to inundation, especially during peak discharge periods or in the absence of adequate flood protection infrastructure. Conversely, areas that are situated farther from rivers fall into the "Low" or "Very Low" vulnerability classes, indicating reduced exposure to fluvial flooding. The findings are consistent with previous studies. For instance, Adeyemi and Komolafe (2025) and Aladejana and Ebijuworih (2024) both emphasized that distance to the river is one of the most influential parameters in flood hazard modeling. Their results also showed that areas closest to rivers consistently exhibited the highest flood risk. Similarly, Kumar et al. (2025) and Rahmati et al. demonstrated

through spatial modeling that proximity to rivers had the strongest correlation with historical flood events across different basins.

In contrast studies such as Al-Kindi and Alabri (2024) caution that although proximity to rivers is crucial, it must be analyzed in conjunction with other factors such as land use, slope, soil permeability, and drainage density to fully understand flood dynamics. This study, however, reaffirms the primacy of river proximity as a standalone indicator, especially in predominantly fluvial flood-prone zones.

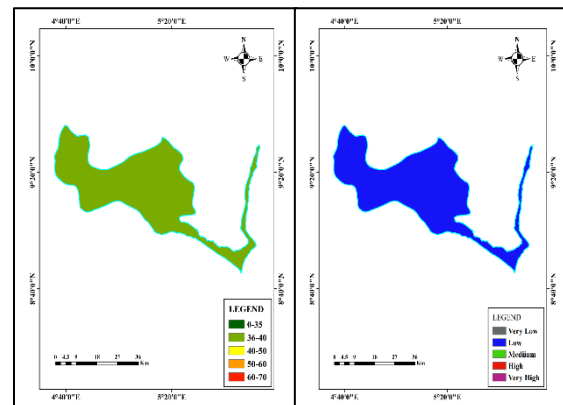


Figure 3: Rainfall map and Reclassified Rainfall map

Figure 3 shows the rainfall map and the reclassified rainfall map. The rainfall map shows spatial variations in annual average rainfall across the study area. On the left panel, the reclassified rainfall intensity is grouped into five classes: 0–35 mm, 36–40 mm, 40–50 mm, 50–60 mm, and 60–70 mm, with higher rainfall values shown in orange and red tones. The right panel converts these rainfall classes into a vulnerability map, where the areas with higher rainfall (50–70 mm) correspond to higher flood vulnerability levels, classified from "Very Low" to "Very High."

From the reclassified vulnerability map, it is evident that a large portion of the study area falls within the "Low" vulnerability class, shown in blue. However, narrow zones along the riverbanks and certain low-lying areas experience relatively higher rainfall and thus are more prone to flooding. The positive correlation between high rainfall zones and higher flood vulnerability aligns with established hydrological principles: the more intense the rainfall over time, the higher the surface runoff, particularly in areas with poor drainage, impermeable surfaces, or low slope gradients. This finding agrees with the conclusions of Umar and Gray (2023), who reported that rainfall is one of the most significant contributors to flood generation, especially in regions with inadequate natural or artificial drainage systems. Similarly, Aliyu et al. (2024) emphasized that areas with high rainfall intensity tend to experience higher flood frequencies and severities, particularly when combined with other vulnerability factors such as poor land cover and low infiltration rates.

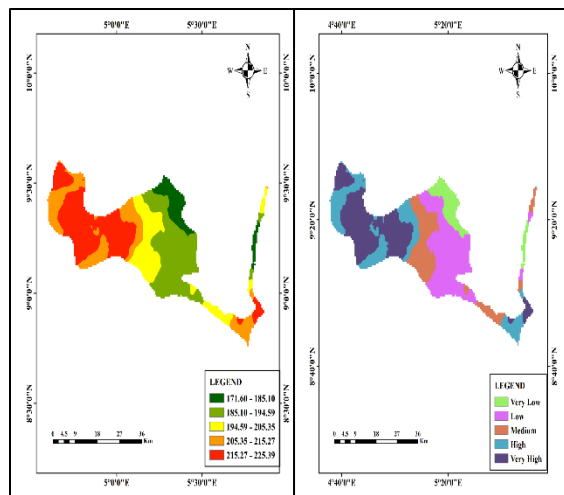


Figure 4: Spatial Distribution of Drainage Density and Its Reclassified Map Showing Vulnerability Levels

Figure 4 shows the drainage density and reclassified drainage density map. The result derived from the drainage density maps provides a significant insight into the spatial relationship between surface hydrological characteristics and flood vulnerability within the study area. This highlights the significant role of drainage patterns in influencing flood risk within the study area. The left panel of the map displays a continuous surface of drainage density values, which range from 171.60 km/km² to 225.39 km/km². These values have been spatially reclassified into five classes on the right panel, corresponding to vulnerability levels: Very Low, Low, Medium, High, and Very High. The reclassified map clearly shows that areas with high drainage density (values between 215.27 – 225.39 km/km²) are mostly located in the western and southeastern parts of the study area and are classified under the “Very High” flood vulnerability category. This indicates that these areas possess a dense and tightly connected drainage network, which tends to facilitate rapid runoff accumulation during heavy rainfall, thereby increasing the likelihood of flooding. Water does not easily infiltrate in such a region water infiltration is limited due to the swift concentration of flow into channels, especially where topography and soil types further limit percolation.

Conversely, areas with low drainage density (171.60 – 185.10 km/km²) appear in the central and northeastern zones, and are categorized under the “Very Low” or “Low” vulnerability classes. These regions likely contain fewer stream channels and more permeable or flat surfaces, which reduce the rate of surface runoff, thereby decreasing the probability of flood occurrence. This spatial pattern reflects a direct and logical correlation: as drainage density increases, flood vulnerability increases due to faster water concentration and reduced infiltration opportunities. This supports the use of drainage density as a critical parameter in flood modeling and early warning systems.

The result is consistent with empirical findings in similar geographical and climatic contexts. For instance: Yusuf et al. (2023), in their study in Anambra State, Nigeria, found that areas with higher drainage density were significantly more susceptible to flooding due to concentrated runoff and reduced infiltration time. Tudunwada and Abbas (2022) showed through GIS-based flood

hazard mapping in Jigawa State, Northern Nigeria that high drainage density was among the top contributing factors to flood-prone zones. Akhter et al. (2025) also demonstrated that drainage density is among the most statistically significant variables in flood susceptibility modeling using machine learning approaches.

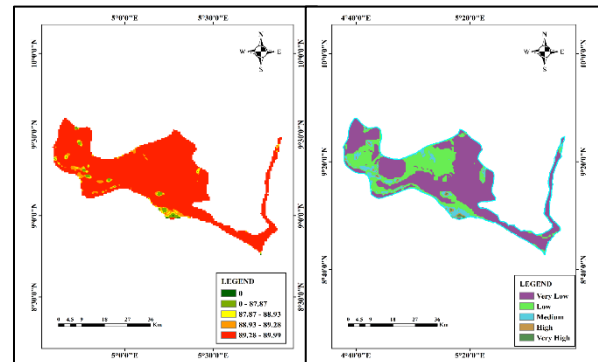


Figure 5: Slope Map and Reclassified Slope Categories

Figure 5 shows the slope and reclassified Slope. The slope maps provided illustrate the spatial variation in terrain gradient and its relationship to flood physical vulnerability across the study area. The left map presents the original slope data, with values ranging from 0 to approximately 89.99 degrees. These values have been reclassified into five classes in the right map, representing levels of flood vulnerability—from “Very Low” (class 1) to “Very High” (class 5). Areas with gentle slopes (near 0 degrees) dominate the region, particularly in the central and southeastern zones, and are predominantly classified under “Very High” and “High” flood vulnerability. In contrast, regions with steeper slopes are mostly found in limited pockets, indicated in red and yellow on the left map, and correspond to “Very Low” or “Low” flood vulnerability on the right map.

This spatial distribution follows a well-established hydrological principle: gentle or flat slopes tend to accumulate and retain surface runoff, thereby increasing the likelihood of water stagnation and flooding, especially during heavy rainfall. Steep slopes, on the other hand, promote rapid surface water flow and drainage, reducing the residence time of water on the surface and thus lowering the probability of flood occurrence. The reclassified slope map clearly captures this pattern, indicating that flatter terrains are more flood-prone due to their limited natural drainage potential. This result aligns with findings from several empirical studies. For instance, Adeyemi and Komolafe (2025) observed that slope was a critical factor in flood hazard modeling lower Niger River basin, Nigeria, with flood susceptibility decreasing as slope increased. Similarly, Ozegin and Ilugbo (2025) found that areas with gentle gradients had higher flood risk due to slower runoff velocities and greater water accumulation. These studies support the results observed in the current map, where flatter regions are consistently categorized as more vulnerable.

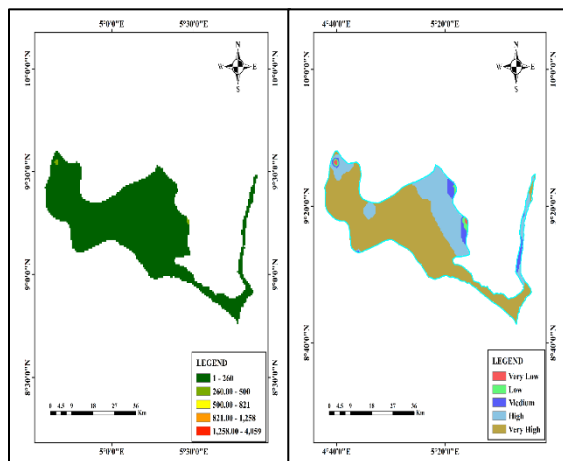


Figure 6: Elevation Map and Reclassified Elevation Map

Figure 6 shows the elevation and reclassified elevation map in the study area. The elevation map in the left panel of the figure shows the spatial variation of elevation values across the study area, ranging from 1 to 4,059 meters. Lower elevations ranging from 1 to 260 metres are illustrated in darker green shades, while higher elevations exceeding 1,258 metres, appear in warmer colours such as yellow and red. Elevation is a critical factor influencing flood vulnerability because it determines how water flows across the terrain—areas at lower elevations are typically more prone to water accumulation, runoff concentration, and inundation.

On the right panel, the elevation values have been reclassified into five categories reflecting flood vulnerability levels. Areas with the lowest elevations are classified as “Very High” vulnerability, whereas the highest elevation zones are categorised as “Very Low” vulnerability. This reclassification reveals that the majority of the flood-prone zones are located in areas of low elevation, particularly along river corridors and valley floors. These zones are highly susceptible to overland flow and surface water pooling during rainfall events. In contrast, areas at higher elevations are less likely to experience floodwaters, as runoff naturally flows away from these elevated surfaces.

This result is consistent with findings from Ahmed et al. (2024), who emphasized that low elevation is one of the most influential parameters in flood hazard mapping. These studies showed that flood risk significantly increases in low-lying terrain, especially in basins where rainfall runoff accumulates rapidly. Additionally, Al-Kindi and Alabri (2024) noted that elevation often inversely correlates with flood risk, particularly in areas lacking adequate drainage systems or with gentle slopes that delay water evacuation.

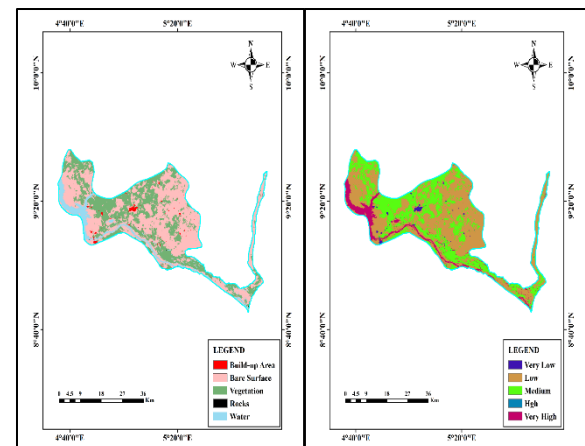


Figure 7: Land Use Land Cover (LULC) Map and Reclassified LULC Map

Figure 7 shows the LULC and Reclassified LULC Map of the study area. The left map presents LULC distribution across the study area, identifying five major land cover classes: water bodies (blue), built-up areas (red), bare surfaces (light pink), vegetation (green), and rocky surfaces (black). Vegetation and bare surfaces dominate the landscape, with built-up areas sparsely distributed, mostly in the central and southern regions. Water bodies are more concentrated along the western and eastern boundaries. In terms of flood physical vulnerability, land cover plays a significant role in surface hydrology. Water bodies and built-up areas are particularly critical: the former indicates existing flood-prone zones, while the latter consists of impervious surfaces that limit infiltration and increase surface runoff. Bare surfaces, though permeable, are often compacted and lack vegetation cover, making them vulnerable to erosion and flash floods. Vegetated areas, on the other hand, provide better infiltration and act as buffers, reducing flood intensity. These findings are supported by studies like that of Alimi et al. (2022), which assert that areas with dense vegetation exhibit significantly lower flood vulnerability than urbanized or barren landscapes.

The right map is a reclassified version of the LULC data, structured to reflect the influence of each land cover type on flood physical vulnerability. It employs a scale from 1 (very low influence) to 5 (very high influence), where vegetation is classified as class 1 due to its flood-mitigating properties, while water bodies are classified as class 5 as they inherently represent flood-prone zones. Built-up areas fall into class 4 due to their impervious nature, and bare surfaces into class 3, reflecting their moderate vulnerability. Rocky surfaces are classified as class 2, offering relatively low—but not negligible—flood influence. The spatial pattern highlights high to very high flood vulnerability (classes 4 and 5) primarily along water channels and urban centers, especially in the west and southeast. The central zone, rich in vegetation, predominantly shows low to very low vulnerability. This classification aligns well with prior research, including Ibitoye et al. (2020), which found that urban and bare surfaces significantly increase flood risks due to reduced permeability and disrupted natural drainage. However, some debate remains regarding rocky areas, while generally resistant to erosion, their flood impact may vary based on topography and soil overlay. Overall, the reclassified map offers a more detailed and insightful approach for evaluating flood risk, emphasizing how

human activity and natural land cover interact to shape local flood vulnerability.

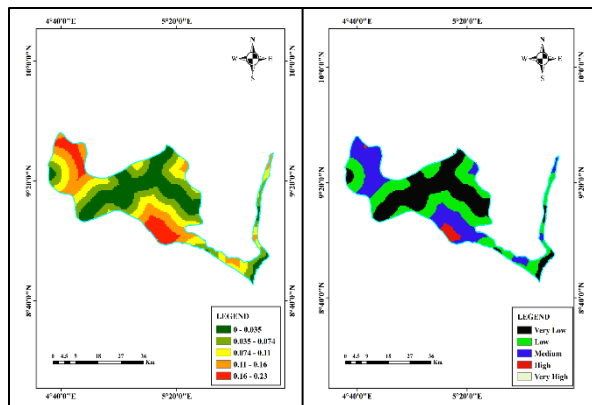


Figure 8: Distance to Road Map and Reclassified Distance to Road Maps

Figure 8 show the spatial distribution of distance to roads and its reclassification within the study area. The left map in the image shows the original Distance to Road data, representing the proximity of different areas to the nearest roads. The values range from 0 to 0.23, where lower values (in dark green) indicate areas very close to roads, and higher values (in red and orange) indicate areas farther away. The spatial distribution reveal that much of the central and northeastern portions of the study area lie in close proximity to roads, whereas the southern and southeastern corners are farther away. In the context of flood vulnerability, proximity to roads can be a double-edged sword. On one hand, roads often alter natural drainage patterns, compact soil, and increase impervious surface coverage, thereby elevating flood risk in adjacent areas. On the other hand, roads also play a vital role in facilitating emergency response and evacuation efforts, thereby helping to mitigate the impacts of flooding. Thus, areas closer to roads—despite the hydrological disadvantages—may also benefit from quicker post-disaster response. Studies such as those by Njoku et al. (2020) note that proximity to roads can increase flood exposure due to altered runoff dynamics, supporting the concern shown in regions with low distance-to-road values on this map.

The right map represents the reclassified version of the Distance to Road data, depicting how distance influences flood physical vulnerability on a scale from 1 (very low influence) to 5 (very high influence). In this classification, areas closer to roads are assigned higher vulnerability classes (e.g., red for “High” and blue for “Medium”), while regions farther away fall into the “Low” and “Very Low” categories (black and green). This reclassification assumes that closer proximity to roads exacerbates flood vulnerability due to the likelihood of disrupted drainage, soil sealing, and infrastructure-induced runoff. The spatial patterns indicate that vulnerability is higher in the southeastern and southwestern zones—areas that were earlier shown to be nearer to road networks—while vulnerability is lower in the central and far eastern regions. This assessment aligns with findings by Caleb and Chioma (2025), who reported that road-adjacent areas are frequently exposed to urban flooding due to inadequate drainage planning and road-induced channeling of stormwater. However, it may diverge from studies emphasizing the resilience-enhancing role of road infrastructure in rural areas, where access is a lifeline during flood events.

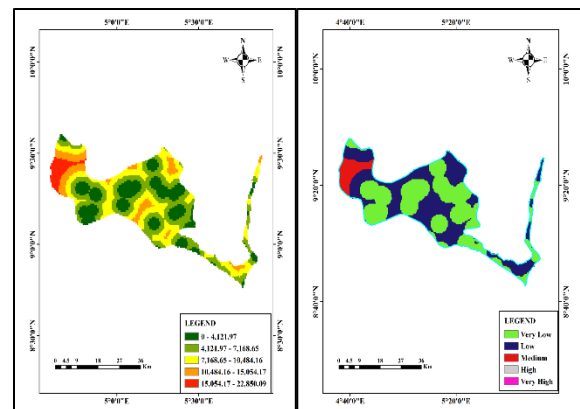


Figure 9: Distance to Build-up Map and Reclassified Distance to Build-up Maps

Figure 9 shows the distance to built-up areas and the corresponding reclassified map for the study area. The two maps—the Reclassified Distance-to-Built-Up Area Map and the Reclassified Flood Physical Vulnerability Map—present a spatial comparison of how human settlement patterns influence flood risk in the study area. Analyzing both maps together allows for a deeper understanding of the role that proximity to built-up areas plays in shaping physical flood vulnerability across the landscape. The left map, the Distance-to-Built-Up Area Map, categorizes the study area into five distance classes based on proximity to existing built-up (urbanized) zones. These distance intervals—ranging from 0 to 22,850.99 meters—were grouped into five classes to simplify analysis and interpretation. Specifically, the first class (0–4,121.97 m) represents areas very close to built-up zones, while the last class (15,054.17–22,850.99 m) includes areas that are farthest from settlements. These classes were reclassified on a scale of 1 to 5, where higher values (5) indicate close proximity to built-up areas, and lower values (1) represent distant, likely rural or undeveloped zones. This classification framework assumes that proximity to human settlements increases exposure to flood risks, which is evident in the corresponding flood physical vulnerability map, where zones closest to built-up areas (5) frequently align with regions of medium to high vulnerability. The rationale behind this relationship lies in the nature of urban development—impervious surfaces in built-up areas prevent water infiltration and increase runoff, while poorly planned drainage systems often exacerbate flooding in these densely developed zones.

The right map, the Reclassified Flood Physical Vulnerability Map, shows how susceptible different areas are to flooding based on a combination of physical and environmental variables, such as topography, land cover, and proximity to both natural and human features. This map uses color-coded categories, ranging from Very Low (blue) to High (red) vulnerability. Spatially, areas identified as having higher flood vulnerability—particularly in the western part of the map—closely correspond to zones classified as very close to built-up areas in the distance map. Conversely, regions with lower flood vulnerability are generally situated farther from settlements and are more likely to be covered with vegetation or located in undisturbed terrain.

Together, the two maps reveal a clear spatial correlation: areas closer to built-up environments are more physically vulnerable to flooding, whereas regions located farther away generally experience lower vulnerability. This trend is explained by the fact that built-up areas often consist of impervious surfaces, such as concrete and asphalt, which inhibit natural infiltration of rainfall. These surfaces generate higher surface runoff during storms, overwhelming drainage systems and increasing flood risks for nearby areas. Furthermore, human settlements tend to encroach on natural waterways or low-lying zones, often without proper hydrological planning, which disrupts the natural flow of water and contributes to localized flooding. In contrast, areas far from human settlements typically feature natural vegetation and permeable soils, both of which help reduce runoff and buffer the impacts of intense rainfall.

The spatial pattern observed in the maps supports findings from various studies in both urban and peri-urban contexts. For example, Salami et al. (2017) report that unregulated urban sprawl and informal settlement expansion in Nigerian cities have significantly increased flood risk in areas surrounding built-up zones. Ifatimehin et al. (2020) likewise identified proximity to settlements as a significant factor influencing flood vulnerability in the floodplains of north-central Nigeria. However, some contrary findings exist. Studies like Effiong et al. (2024) noted that not all urban areas are highly vulnerable, especially where proactive measures—such as well-designed drainage infrastructure, elevated construction, and land-use zoning—are implemented. This suggests that while proximity to built-up areas generally increases vulnerability, this relationship can be moderated by the quality of urban planning and infrastructure.

Figure 10 presents the clay content and its reclassified version. The two maps—the Clay Content Map (left) and the Reclassified Flood Physical Vulnerability Map (right)—together provide a detailed spatial understanding of how soil texture, particularly clay concentration, influences flood risk in the study area. The Clay Content Map illustrates the distribution of clay across the landscape, with values ranging from 3.04 to 9.37. Areas with higher clay content—depicted in red and orange shades—are concentrated in the southern and southeastern parts of the study area, while regions in the north and northeast show lower clay values (green to yellow). High clay content signifies low soil permeability and high-water retention, meaning rainfall is less likely to infiltrate the ground. Instead, it generates greater surface runoff, leading to waterlogging and flooding, especially in flat or poorly drained areas. Therefore, the spatial concentration of clay is a key factor contributing to flood hazards.

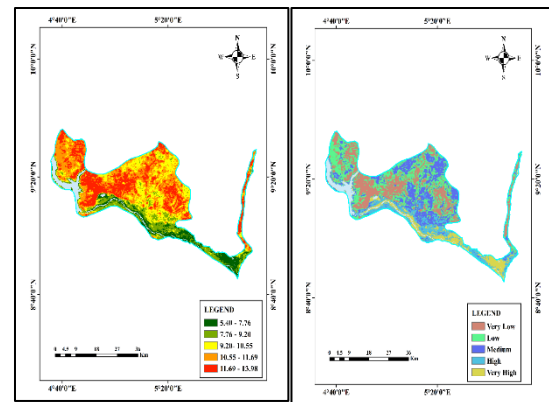


Figure 10: Clay Content Map and Reclassified Flood Physical Vulnerability Based on Clay Content

The reclassified flood map, on the right, divides the landscape into five categories of flood risk—from Very Low (cyan) to Very High (dark blue). Notably, areas of High and Very High vulnerability are predominantly located in the southern and central zones, which spatially correspond with the high-clay regions identified in the clay content map. This pronounced spatial correlation indicates that clay-rich soils play a significant role in amplifying flood vulnerability. Conversely, areas with low clay content primarily in the northwest and northeast—are generally classified as Low or Very Low in terms of flood vulnerability, suggesting better natural drainage and higher soil permeability in these areas. However, the vulnerability map also incorporates other critical factors such as slope, elevation, land use, and proximity to water bodies, which explains why some areas with moderate clay content still fall into medium or high vulnerability classes, highlighting the multifactorial nature of flood risk.

The patterns observed in both maps are consistent with findings from numerous hydrological studies. Researchers such as Adelana (2024) and Ozegin and Ilugbo (2025) have emphasized that clayey soils significantly reduce infiltration and increase flood potential. These findings affirm that clay content is not only a standalone flood driver but also a significant component within broader flood vulnerability assessments.

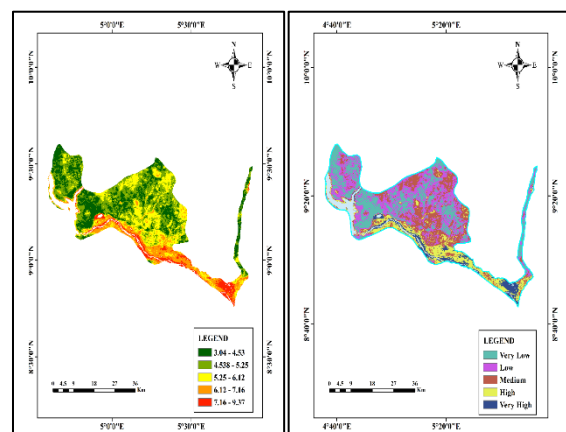


Figure 11: Sand Content Map and Reclassified Sand Content Maps

Figure 10 show the sand content and reclassified sand content maps. The two maps provided represent sand distribution (left) and its reclassification based on its influence on flood physical vulnerability (right). Each map offers a spatial insight into the role of sand content in modulating the landscape's susceptibility to flooding, which is an essential component of comprehensive flood risk assessment. The first map (left) illustrates the spatial distribution of sand content across the study area. The sand content ranges from 5.40% to 13.98%, with a clear gradation from green (low sand content) to red (high sand content). The central and northwestern portions of the region are predominantly shaded in red and orange tones, indicating high sand content, in contrast the southern and southeastern regions are characterised by lower sand content, represented by green tones.

In the context of flood vulnerability, areas with higher sand content generally have greater infiltration capacity, which tends to reduce surface runoff and thus may lower flood risk. However, in some cases, particularly in flat terrain, sandy soils can also become saturated quickly, reducing infiltration efficiency and contributing to local flooding. The map provides a foundational geotechnical context for interpreting flood vulnerability but does not directly link sand content to flood hazard levels.

The second map (right) is a reclassified version of the sand distribution map, categorizing areas based on the degree of influence of sand content on flood physical vulnerability. This map uses a five-class scale: from 1 (Very Low) to 5 (Very High) influence. Interestingly, the regions with low sand content (from the first map) are now assigned with higher influence values (4&5) in the reclassified vulnerability map, particularly across the southern and southeastern. This suggests that low sand content correlates with higher flood vulnerability, likely due to poor drainage and higher runoff potential. Conversely, areas with high sand content are mostly reclassified into lower influence categories (1 and 2), supporting the understanding that sandier areas tend to be less vulnerable to floods due to better permeability.

These observations are consistent with previous studies. For example, a study by Oturo et al. (2024) in southwestern Nigeria highlighted that sandy soils are generally associated with lower flood risk due to their higher infiltration capacity. In contrast, Chinedu et al. (2024) found that areas with lower sand content exhibited increased surface water retention and higher flood incidences. The findings shown in these maps align well with such studies, strengthening their reliability. However, in some deltaic environments or areas with compacted sandy layers, exceptions have been noted, where sand-rich soils still experienced localized flooding due to topography or land cover modifications—this nuance should be noted when generalizing the results.

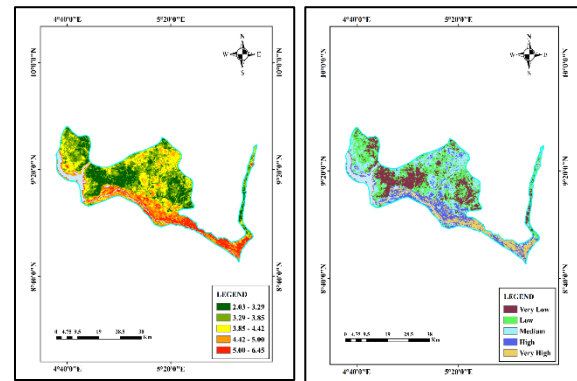


Figure 12: Silt Content Map and Reclassified Silt Content Maps

Figure 12 shows the silt content and reclassified silt content maps of the study area. The two maps presented illustrate the spatial variation of silt content and its influence on flood physical vulnerability across the study area. The first map shows the actual distribution of silt, with values ranging from 2.03% to 6.45%. Higher silt concentrations, represented by red and orange shades, are mainly found in the southern and southeastern parts of the region, indicating zones of potential sediment deposition and reduced infiltration capacity. These areas are often more prone to flooding due to the fine texture of silt, which tends to compact and reduce the soil's ability to absorb water, thus increasing surface runoff. In contrast, the central and northern regions, shaded green and yellow, exhibit lower silt content, suggesting better drainage conditions and relatively lower flood susceptibility.

The second map presents a reclassified version of silt content, illustrating its influence on flood vulnerability, using a five-class scale where 1 represents very low influence and 5 represents very high influence. In this reclassified map, areas with high silt content from the first map are now predominantly categorized under high and very high influence classes. This reclassification confirms that silt content is a significant factor contributing to flood risk, especially in areas where natural drainage is poor. The map highlights that low-lying or depositional regions with high silt accumulation are more vulnerable to flood events due to the reduced permeability and delayed infiltration caused by the fine soil particles.

These findings are consistent with several other studies. For instance, Chinedu et al. (2024) reported that silt-dominated soils in southwestern Nigeria contributed significantly to urban flooding due to their low infiltration rates. Similarly, Ozegin and Iugbo (2025) found that communities located on silt-rich floodplains in Nigeria experienced frequent flood events, emphasizing the role of soil texture in flood hazard mapping. In a related study, Abah and Petja (2017) emphasized that elevated silt levels in riverine areas of the Lower Benue Basin heightened flood risk, particularly during peak rainfall months. The spatial relationship depicted in these maps corroborates earlier findings, further substantiating the argument that elevated silt content contributes significantly to heightened flood physical vulnerability.

Overall, both maps serve as important tools for flood risk assessment and can guide planning decisions aimed at reducing

vulnerability in silt-prone areas.

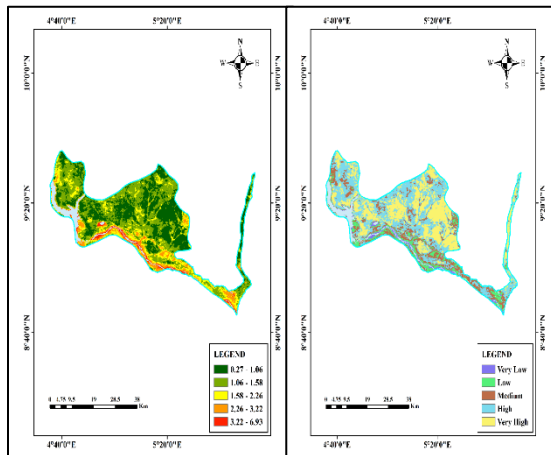


Figure 13: Soil Organic Carbon (SOC) Map and Reclassified SOC Map

Figure 13 shows the SOC and Reclassified SOC maps of the study area. The first map on the left illustrates the spatial distribution of SOC across the study area, with values ranging from 0.27 to 6.93. The color gradient from green to red represent increasing SOC content, with green areas representing low SOC and red areas indicating high SOC levels. Notably, higher SOC values are concentrated in the southern and southeastern parts of the region, while lower values are more prevalent in the northern and some southwestern zones. From a hydrological standpoint, higher SOC levels generally enhance soil structure, improve water infiltration,

Table 1: Criteria Weights of the Nine Variables

Key= Soil Organic Carbon (SOC), Distance to Road (DRD), Land Use/Land Cover (LULC), Elevation (ELV), Slope (SLP), Rainfall (RF), Drainage

S/N	Criteria	Calculated Weight
1	Soil Organic Carbon (SOC)	0.041
2	Distance to Road (DRD)	0.072
3	Land Use/Land Cover (LULC)	0.198
4	Elevation (ELV)	0.168
5	Slope (SLP)	0.129
6	Rainfall (RF)	0.148
7	Drainage Density (DD)	0.101
8	Distance to Built-Up (DB)	0.061
9	Distance to River (DR)	0.082

and increase moisture retention, all of which contribute to reducing surface runoff and mitigating flood risk. Therefore, areas with high SOC values in this map may be inherently more resilient to flooding. This result aligns with findings by Akpoveta et al. (2014), who emphasize that high SOC enhances soil's capacity to absorb water, thereby playing a critical role in flood prevention. On the other hand, areas with low SOC are likely to have poor infiltration and increased runoff, making them more susceptible to flood hazards.

The second map on the right presents a reclassified version of the SOC data, categorizing it into five classes based on its influence on flood physical vulnerability. Here, SOC values have been translated into vulnerability levels, with class 1 (blue) indicating very low influence on flood vulnerability—implying greater resilience—and class 5 (yellow) indicating very high influence—signifying higher susceptibility to flooding. This classification reveals that areas in the northern and central parts, which had higher SOC in the first map, fall under classes 1 and 2, indicating lower flood vulnerability. In contrast, southern and southeastern areas, previously shown to have moderate to low SOC, are now classified under classes 4 and 5, suggesting high flood vulnerability. This transformation provides a clearer understanding of how SOC directly influences flood risks. The reclassified map supports findings by Alaoui et al. (2018), who argue that low SOC levels lead to soil compaction and poor infiltration, thereby exacerbating flood risks. While this approach effectively visualizes the relationship between SOC and flood vulnerability, it is important to acknowledge that flood risk is influenced by multiple interacting factors. Topography, rainfall intensity, and land use practices also play crucial roles and may influence the accuracy of SOC-based vulnerability assessments. Nonetheless, the reclassified map offers a valuable tool for integrating soil data into flood risk management strategies.

Density (DD), Distance to Built-Up (DB) and Distance to River (DR)

λ_{max} : 9.00

Consistency Index (CI): 0.000

Random Index (RI): 1.45

Consistency Ratio (CR): 0.000

Table 1 presents the assigned weights for the nine criteria used in the analysis. The results presented in the table offer a systematic evaluation of flood vulnerability drivers using expert-informed criteria weights. The most influential factors in this assessment were Land Use/Land Cover (LULC) with a weight of 0.198, followed by Elevation (0.168) and Rainfall (0.148). These factors reflect the primary geophysical and environmental elements that shape flood dynamics in Mokwa, Niger State. Land use influences surface runoff and infiltration capacity, elevation controls the flow path and accumulation zones, and rainfall acts as the direct hydrological trigger for flooding.

Moderately weighted factors such as Slope (0.129), Drainage Density (0.101), and Distance to River (0.082) are equally vital. Steeper slopes can accelerate runoff, while areas closer to rivers tend to be more prone to inundation. Drainage density, which reflects the extent to which an area is dissected by streams and rivers, influences water retention and surface runoff accumulation. Distance to Road (0.072) and Distance to Built-Up Area (0.061) exhibit relatively lower, yet still significant, influence, primarily due to anthropogenic modification of drainage patterns and the vulnerability of infrastructure. The Soil Organic Carbon (SOC) factor, with the lowest weight (0.041), reflects its indirect role in

flood risk, primarily affecting soil structure and erosion rather than flood volume or flow directly.

The consistency of these judgments was validated using the internal validation metrics of the Analytic Hierarchy Process (AHP). A Consistency Index (CI) of 0.000 and a Consistency Ratio (CR) of 0.000 (with $\lambda_{\text{max}} = 9.00$ and $RI = 1.45$ for $n = 9$) indicate perfect consistency in the pairwise comparisons, suggesting highly logical and proportional decision-making across the criteria. This weighting scheme aligns closely with findings in several related studies. For instance, Adeyemi and Komolafe (2025) emphasized LULC and elevation as dominant in determining flood vulnerability in the Niger River basin. Similarly, Tiepolo and Galligari (2021) highlighted the influence of rainfall patterns and slope steepness in flood-prone urban and peri-urban zones in central Nigeria.

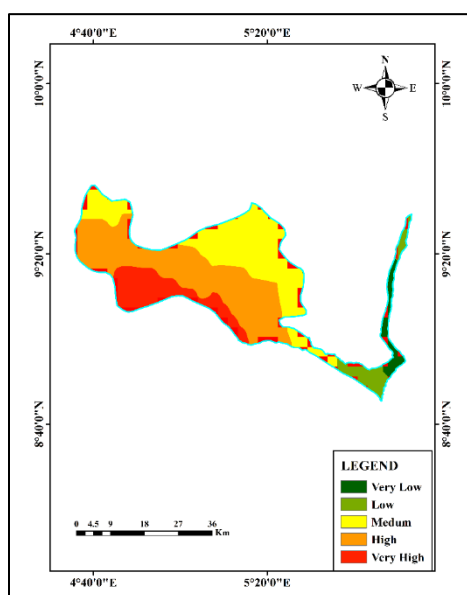


Figure 14: Physical Vulnerability Map

The physical vulnerability map is presented in figure 13. The figure shows the spatial distribution of flood vulnerability across the study area, categorized into five classes: Very Low, Low, Medium, High, and Very High. The classification shows a clear gradient from the eastern to the western parts of the region. The eastern flank, particularly along the narrow stretch bordering water bodies, exhibits predominantly "Very Low" to "Low" vulnerability (shaded in dark and light green), suggesting higher elevation, more effective drainage, or distance from flood-prone rivers. In contrast, the central and western areas are dominated by "High" and "Very High" vulnerability zones (orange and red), likely due to lower elevation, higher drainage density, and proximity to rivers or poorly drained basins.

This spatial pattern aligns with topographic influences, where lower-lying and flatter terrains often correlate with higher flood susceptibility. The central convergence of "High" and "Very High" classes also indicates potential flood basins or areas of runoff accumulation, especially in regions with compromised soil infiltration capacity or intensive land use activities such as agriculture and urbanization. Comparatively, the findings resonate with studies such as Umar and Gray (2023), who identified that flood vulnerability is often higher in low-lying and densely populated

zones of Nigeria, where drainage infrastructure is either inadequate or poorly maintained. Similarly, Alimi et al. (2022) noted that areas with poor topographic slope and high rainfall intensity, especially around urban fringes, are more exposed to flood hazards.

Table 2: Spatial Distribution of Flood Vulnerability Classes and Area Coverage in the Study Area (km²)

S/N	Degree of Vulnerability	Area Covered KM3
1	Very Low	223
2	Low	303
3	Medium	1473
4	High	1624
5	Very High	516
Total		4139

Table 2 presents the spatial distribution of flood vulnerability classes along with their corresponding area coverage (in km²) across the study area. The tabulated data provides valuable insight into the spatial extent of each flood vulnerability class across the study area, totaling 4,139 km². The analysis of the area covered by each class reveals a significant variation in vulnerability distribution, which is crucial for targeted planning and intervention. The "High" vulnerability class occupies the largest area, covering approximately 1,624 km², which constitutes nearly 39.2% of the total study area. This indicates that a substantial portion of the landscape is highly susceptible to flooding, likely due to a combination of physical factors such as proximity to water bodies, low elevation, gentle slopes, as well as anthropogenic influences, including deforestation and inappropriate land use practices.

Following closely is the "Medium" vulnerability class, which occupies around 1,473 km² or 35.6% of the study area, indicating a considerable extent of moderate flood risk. This suggests that over one-third of the region is moderately at risk, which could escalate to high vulnerability with changes in rainfall patterns or increased human activity. The widespread distribution of this class highlights the transitional nature of vulnerability across the landscape. The "Very High" vulnerability class spans 516 km², accounting for 12.5% of the total area. This zone represents critical hotspots where flood risk is most severe. These areas should be prioritized for mitigation efforts, infrastructure reinforcement, early warning systems, and potentially relocation strategies if settlements are present. On the lower end, the "Low" vulnerability class covers 303 km² (7.3%), while the "Very Low" class occupies the smallest area, 223 km² (5.4%). These zones are likely situated on higher elevations or areas with better natural drainage and less exposure to direct runoff or river overflow. While they are relatively safe, they still require monitoring, especially in the face of climate change and land use dynamics. This distribution shows that over 87% of the land area falls under medium to very high vulnerability, underscoring the urgent need for integrated flood control measures. The data supports the development of adaptive land use planning, improved drainage systems, afforestation programs, and community-based resilience initiatives in the most vulnerable zones.

Conclusion

This study conducted an integrated geospatial and multi-criteria evaluation of flood physical vulnerability in Mokwa Local Government Area, Niger State, Nigeria. Using eleven physical and

anthropogenic variables—such as elevation, slope, rainfall, drainage density, proximity to rivers and roads, land use/land cover (LULC), and soil properties including sand, silt, clay, and soil organic carbon (SOC)—the research generated reclassified thematic layers and a composite vulnerability map. Each factor was individually assessed for its influence on flood risk and synthesized using the Analytical Hierarchy Process (AHP) to assign appropriate weights. The findings highlight that flood vulnerability in the study area is driven by a combination of natural terrain features and human-induced land alterations. Areas with low elevation, gentle slopes, high rainfall, dense drainage networks, proximity to rivers and built-up areas, and clay-rich soils were identified as highly vulnerable to flooding, while those with sandy soils, higher elevation, extensive vegetation, and high SOC exhibited lower susceptibility due to better drainage and infiltration capacity. The AHP analysis showed that LULC (0.198), Elevation (0.168), and Rainfall (0.148) were the most influential parameters, with one model yielding a perfect consistency ratio (CR = 0.000) and another within acceptable limits (CR = 0.107), reinforcing the significant impact of both natural and anthropogenic factors in shaping flood dynamics. The composite vulnerability map categorized the landscape into five classes: Very Low, Low, Medium, High, and Very High. Notably, 39.2% of the area was classified as High vulnerability and 35.6% as Medium, while 12.5% fell into the Very High category, predominantly in the central and western zones—together accounting for over 87% of the landmass being moderately to severely at risk of flooding. These results are consistent with previous studies that highlight the significant role of river proximity, land use changes, and terrain characteristics in determining flood susceptibility. Still, this research further contributes by integrating soil characteristics—often neglected in similar assessments—into the vulnerability framework. From a policy and planning perspective, the study recommends preventing new developments in High and Very High risk zones, enhancing flood-resilient infrastructure such as drainage systems in urban and road-adjacent areas, promoting soil conservation through afforestation and organic matter enrichment, instituting early warning systems and community preparedness programs, and embedding geospatial flood risk data into land use and development planning. Ultimately, the study illustrates the critical importance of coupling geospatial analysis with decision-support tools like AHP for a comprehensive understanding of flood risk. As climate variability and land use pressures intensify, such integrative methods are vital for evidence-based planning, disaster risk reduction, and sustainable environmental governance in flood-prone regions like Mokwa and beyond.

REFERENCES

- Abah, Roland Clement, and Brilliant Mareme Petja. 2017. "Increased Streamflow Dynamics and Implications for Flooding in the Lower River Benue Basin." *African Journal of Environmental Science and Technology* 11(10):544–55. doi: 10.5897/AJEST2015.2069.
- Abrate, Tommaso, Pierre Hubert, and Daniel Sighomnou. 2013. "A Study on Hydrological Series of the Niger River." *Hydrological Sciences Journal* 58(2):271–79. doi: 10.1080/02626667.2012.752575.
- Adelana, A. O. 2024. "Urban Soil Infiltration Rates on Different Land Use Types in Southwest Nigeria: Actual versus Model Estimates." *LAUTECH Journal of Engineering and Technology* 18(3). doi: 10.36108/laudet/4202.81.0320.
- Adeyemi, Adedoyin Benson, and Akinola Adesuji Komolafe. 2025. "Flood Hazard Zones Prediction Using Machine-Learning-Based Geospatial Approach in Lower Niger River Basin, Nigeria." *Natural Hazards Research* 5(2):399–412. doi: 10.1016/j.nhres.2025.01.002.
- Ahmed, Istak, Nibedita Das (Pan), Jatan Debnath, Moujuri Bhowmik, and Shaswati Bhattacharjee. 2024. "Flood Hazard Zonation Using GIS-Based Multi-Parametric Analytical Hierarchy Process." *Geosystems and Geoenvironment* 3(2):100250. doi: 10.1016/j.geogeo.2023.100250.
- Akhter, Shapla, Md. Mostafizur Rahman, and Md. Moniruzzaman Monir. 2025. "Flood Susceptibility Analysis to Sustainable Development Using MCDA and Support Vector Machine Models by GIS in the Selected Area of the Teesta River Floodplain, Bangladesh." *HydroResearch* 8:127–38. doi: 10.1016/j.hydres.2024.10.004.
- Akoji, Solomon John, Friday Christopher Rintep, and Sarah Itse Anya. 2025. "Socioeconomic Uncertainties and Food Crisis in Nigeria: Current Obstacles and Future Opportunities." *African Journal of Management and Business Research* 19(1):275–90. doi: 10.62154/ajmbr.2025.019.01023.
- Akpoveta, Vincent O., Steven A. Osakwe, Osaro K. Ize-Iyamu, Weltime O. Medjor, and Felix Egharevba. 2014. "Post Flooding Effect on Soil Quality in Nigeria: The Asaba, Onitsha Experience." *Open Journal of Soil Science* 04(02):72–80. doi: 10.4236/ojss.2014.42010.
- Al-Kindi, Khalifa M., and Zahra Alabri. 2024. "Investigating the Role of the Key Conditioning Factors in Flood Susceptibility Mapping Through Machine Learning Approaches." *Earth Systems and Environment* 8(1):63–81. doi: 10.1007/s41748-023-00369-7.
- Aladejana, Olabanji Odunayo, and Etari Joy Ebijuworih. 2024. "Flood Risk Assessment in Kogi State Nigeria through the Integration of Hazard and Vulnerability Factors." *Discover Geoscience* 2(1):31. doi: 10.1007/s44288-024-00036-y.
- Alaoui, Abdallah, Magdalena Rogger, Stephan Peth, and Günter Blöschl. 2018. "Does Soil Compaction Increase Floods? A Review." *Journal of Hydrology* 557:631–42. doi: 10.1016/j.jhydrol.2017.12.052.
- Alhaji, Mohammed. 2022. "Flood Vulnerability Assessment in the Gbako River." *African Scholar Journal of Built Env. & Geological Research* 26(4):101–8.
- Alimi, S. A., T. W. Andongma, O. Ogungbade, S. S. Senbore, V. C. Alepa, O. J. Akinlabi, L. O. Olawale, and Q. O. Muhammed. 2022. "Flood Vulnerable Zones Mapping Using Geospatial Techniques: Case Study of Osogbo Metropolis, Nigeria." *The Egyptian Journal of Remote Sensing and Space Sciences* 25(3):841–50. doi: 10.1016/j.ejrs.2022.08.003.
- Aliyu, Zakaria, Ibrahim Mukhtar, Suleiman Abdulkadir, and Muhammad Hamza. 2024. "Multi-Criteria Analysis and Mapping of the Vulnerable Flood Risk Areas of Jigawa State, Nigeria." *Dutse Journal of Pure and Applied Sciences (DUJOPAS)* 10(3):39–54.
- Baba, Bashariya Mustapha., Zaharaddeen. Isa, Auwal Faruq Abdussalam, and Babati. Abu-hanifa. 2022. "Modelling

- The Signature Of Human Influence On Vegetation Dynamic In Kamuku National Park , Nigeria." *Science World Journal* 17(2):234–47.
- Baba, Bashariya Mustapha, Zaharaddeen Isa, Auwal Faruq Abdussalam, and Abu-Hanifa Babati. 2022. "Influence Of Climate Indices On Vegetation Dynamics In Kamuku National Park, Nigeria Using Coupled Model Intercomparison Project Phase 6 (CMIP6)." *FUDMA Journal of Sciences* 6(4):160–73. doi: <https://doi.org/10.33003/fjs-2022-0604-1059> 8 FJS.
- Babati, A. H., Auwal Farouk Abdussalam, Saadatu Umaru Baba, Zaharaddeen Isa, and Adamu Yunusa Ugya. 2025. "A Comprehensive Review of Flood Monitoring and Evaluation in Nigeria." *International Journal of Energy and Water Resources*. doi: 10.1007/s42108-025-00356-w.
- Babati, Abu-Hanifa, Auwal F. Abdussalam, Saadatu Umaru Baba, and Zaharaddeen Isa. 2022. "Prediction of Flood Occurrences and Magnitude in Hadejia-Jama'are River Basin, Nigeria." *Sustainable Water Resources Management* 8(6):188. doi: 10.1007/s40899-022-00781-3.
- Bello, A. A., M. A. Abua, S. A. Yelwa, F. A. Undiyaundeye, A. I. Iwara, M. A. Abutunghe, B. J. Bassey, D. E. Egbonyi, and S. O. Owalom. 2022. "Geospatial Mapping of Areas at Risk to Flood along Sokoto-Rima River Basin, Sokoto Nigeria." *Environment and Ecology Research* 10(6):806–23. doi: 10.13189/eer.2022.100615.
- Caleb, H., and B. Chioma. 2025. "Architectural Strategies and Risk of Perennial Pluvial Flooding in Port-Harcourt Metropolis." *International Journal of Innovative Scientific & Engineering Technologies Research* 13(1):163–89. doi: 10.5281/zenodo.15058721.
- Chinedu, Ani D., Nkiruka M. Ezebube, Smart Uchegbu, and Vivian A. Ozorme. 2024. "Integrated Assessment of Flood Susceptibility and Exposure Rate in the Lower Niger Basin, Onitsha, Southeastern Nigeria." *Frontiers in Earth Science* 12. doi: 10.3389/feart.2024.1394256.
- Chumky, Tahmina, Mittika Basu, Kenichiro Onitsuka, Gulsan Ara Parvin, and Satoshi Hoshino. 2022. "Disaster-Induced Migration Types and Patterns, Drivers, and Impact: A Union-Level Study in Bangladesh." *World Development Sustainability* 1:100013. doi: 10.1016/j.wds.2022.100013.
- Cirella, Giuseppe T., and Felix O. Iyalomhe. 2018. "Flooding Conceptual Review: Sustainability-Focalized Best Practices in Nigeria." *Applied Sciences* 8(9):1558. doi: 10.3390/app8091558.
- Effiong, Cyril, Eric Ngang, and Idibeke Ekott. 2024. "Land Use Planning and Climate Change Adaptation in River-Dependent Communities in Nigeria." *Environmental Development* 49:100970. doi: 10.1016/j.envdev.2024.100970.
- Gacu, Jerome, Sameh Kantoush, Rodol Candelario, Jessabel Falcuán, Karl Venz Moaje, Mark Jezreel Famaran, Marlo Nepomuceno, Jezzel Anne Ebon, Reniel Parungao, Ryan Ignacio, Marinelle Merida, Perly May Pastrana, and Eduardo Quinton. 2025. "Integrated Multi-Hazard Risk Assessment under Compound Disasters Using Analytical Hierarchy Process (AHP)." *Heliyon* 11(11):e43173. doi: 10.1016/j.heliyon.2025.e43173.
- Ibitoye, Matthew Olomolatan, Akinola Adesuji Komolafe, Abdul-Azeez Suleiman Adegboyega, Abiodun Olufemi Adebola, and Oluwadamilola Daniel Oladeji. 2020. "Analysis of Vulnerable Urban Properties within River Ala Floodplain in Akure, Southwestern Nigeria." *Spatial Information Research* 28(4):431–45. doi: 10.1007/s41324-019-00298-6.
- Ifatimehin, O. O., P. S. U. Eneche, and N. A. Ismail. 2020. "Flood Vulnerability Assessment of Settlements in the Niger-Benue Trough , Central Nigeria." *International Journal of Environment and Climate Change* 10(11):50–67. doi: 10.9734/IJECC/2020/v10i1130266.
- Isa, Zaharaddeen, Auwal F. Abdussalam, Bulus Ajiya Sawa, Muktar Ibrahim, Umar Abdulkadir Isa, and Abu-Hanifa Babati. 2023. "Identifying Major Climate Extreme Indices Driver of Stream Flow Discharge Variability Using Machine Learning and SHaply Additive Explanation." *Sustainable Water Resources Management* 9(4):119. doi: 10.1007/s40899-023-00897-0.
- Isukuru, Efe Jeffery, James Odafe Opha, Obaro Wilson Isaiah, Blessing Orovwighose, and Stephen Sunday Emmanuel. 2024. "Nigeria's Water Crisis: Abundant Water, Polluted Reality." *Cleaner Water* 2:100026. doi: 10.1016/j.clwat.2024.100026.
- Jidauna, G. G., S. R. Barde, C. Ndabula, C. Y. Oche, and D. .. Dabi. 2017. "Water Quality Assessment Of Selected Domestic Water Sources In Dutsinma Town , Katsina State." *Science World Journal* 12(4):43–50.
- Kumar, Kanneganti Bhargav, Shailza Sharma, Rajarshi Das Bhowmik, and P. P. Mujumdar. 2025. "Spatial Synchronization of River Floods Growing beyond the Basin Boundaries in Peninsular India." *Scientific Reports* 15(1):18160. doi: 10.1038/s41598-025-02922-y.
- M.R. Egigogo. 2025. "Day after Devastating Disaster, NEMA Engages Niger Stakeholders on Flood Preparedness." *Premium Times*.
- Musa, A. S., B. R. Atiyong, Z. Isa, A. L. Tanko, and A. Babati. 2022. "Spatio-Temporal Variations Of Soil Salinity In Gusau Local Government Area, Zamfara State, Nigeria." *Fudma Journal Of Sciences* 6(5):109–14. doi: 10.33003/fjs-2022-0605-1108.
- Musa, Hauwa Mohammad Nda, Mohammad Yamman Usman, Husaini Abdul, and Lekan Mohammed Sanni. 2015. "An Assessment of Flood Vulnerability on Physical Development along Drainage Channels in Minna, Niger State, Nigeria." *African Journal of Environmental Science and Technology* 9(1):38–46. doi: 10.5897/AJEST2014.1815.
- Mustapha Baba, Bashariya, Zaharaddeen Isa, Auwal Faruq Abdussalam, and Abu-Hanifa Babati. 2022. "Influence Of Climate Indices On Vegetation Dynamics In Kamuku National Park, Nigeria Using Coupled Model Intercomparison Project Phase 6 (CMIP6)." *FUDMA Journal Of Sciences* 6(4):160–73. doi: 10.33003/fjs-2022-0604-1059.
- Muzzamil, Syed, Hussain Shah, Zahiraniza Mustaffa, Fang Yenn, Mansoor Abdul, Hamid Imam, Khamaruzaman Wan, Ebrahim Hamid, and Hussein Al-qadami. 2020. "A

- Review of the Flood Hazard and Risk Management in the South Asian Region , Particularly Pakistan." *Scientific African* 10:e00651. doi: 10.1016/j.sciaf.2020.e00651.
- Nagya, Abubakar, Umar Kuso, and Muhammad Muhammad. 2024. "Adaptation Initiatives to Flood Risks in the Downstream Section of River Niger Flood Plain in Mokwa Local Government Area of Niger State." *International Journal of Strategic Research in Education, Technology & Humanities*, November 23, 83–101.
- Ndanusa, Z. A., I. J. Musa, A. A. Hudu, And A. Isama'il. 2022. "Multi-Dimensional Model For Flood Vulnerability Assessment In Mokwa: A Case Of Downstream Communities Of Kainji Dam, Niger State, Nigeria." *Journal Of Inclusive Cities And Built Environment* 2(3):69–86. doi: 10.54030/2788-564X/2022/v2s3a6.
- Njoku, Chukwudi Gbadebo, Joel Efiog, and Nse-Abasi Ndiyo Ayara. 2020. "A Geospatial Expose of Flood-Risk and Vulnerable Areas in Nigeria." *International Journal of Applied Geospatial Research* 11(3):87–110. doi: 10.4018/IJAGR.20200701.0a1.
- Odekunle, T. O. 2004. "Rainfall and the Length of the Growing Season in Nigeria." *International Journal of Climatology* 24(4):467–79. doi: 10.1002/joc.1012.
- Okorafor, Okore O., and Maxwell I. Chikwue. 2021. "Mapping Of Flood Prone Areas In Imo State , Southeastern Nigeria Using Gis Techniques." *Scientific Research Journal* 9(7):1–9. doi: 10.31364/SCIRJ/v9.i07.2021.P0721867.
- Olamilekan, Ridwan, Valentine Chidalu Okeke, Nwachukwu Promise Chris, and Chinonye Kamsi Dike. 2024. "Public Health Impacts of Flooding : A Case Study of 2022 Flood Outbreak in Nigeria ." *Int J Travel Med Glob Health* 12(3):145–53. doi: 10.30491/ijtmgh.2024.433930.1400.
- Otuaro, Ebierni Akpoebidimiyen, John Jiya Musa, Abayomi Ibrahim Kuti, Daniel Enebojojo Sunday, and Abdulraheem Gana Muhammad. 2024. "Determination of Infiltration Rate in Developed Areas of Minna, Nigeria." *OALib* 11(04):1–12. doi: 10.4236/oalib.1111471.
- Ozegin, Kesyton Oyamenda, and Stephen Olubusola Ilugbo. 2025. "Evaluation of Potentially Susceptible Flooding Areas Leveraging Geospatial Technology with Multicriteria Decision Analysis in Edo State, Nigeria." *Natural Hazards Research* 5(1):109–33. doi: 10.1016/j.nhres.2024.07.002.
- Salami, Rafiu O., Jason K. von Meding, and Helen Giggins. 2017. "Vulnerability of Human Settlements to Flood Risk in the Core Area of Ibadan Metropolis, Nigeria." *Jamba: Journal of Disaster Risk Studies* 9(1). doi: 10.4102/JAMBA.V9i1.371.
- Singh, Harman, Miriam Nielsen, and Helen Greatrex. 2023. "Causes, Impacts, and Mitigation Strategies of Urban Pluvial Floods in India: A Systematic Review." *International Journal of Disaster Risk Reduction* 93:103751. doi: 10.1016/j.ijdrr.2023.103751.
- Tiepolo, Maurizio, and Andrea Galligari. 2021. "Urban Expansion-Flood Damage Nexus: Evidence from the Dosso Region, Niger." *Land Use Policy* 108:105547. doi: 10.1016/j.landusepol.2021.105547.
- Tudunwada, Ibrahim Yakubu, and Ahmad Abbas. 2022. "Flood Vulnerability Mapping and Prediction for Early Warning in Jigawa State, Northern Nigeria, Using Geospatial Techniques." *International Journal of Disaster Risk Reduction* 79:103156. doi: 10.1016/j.ijdrr.2022.103156.
- Umar, Nura, and Alison Gray. 2023. "Flooding in Nigeria: A Review of Its Occurrence and Impacts and Approaches to Modelling Flood Data." *International Journal of Environmental Studies* 80(3):540–61. doi: 10.1080/00207233.2022.2081471.
- Yusuf, S. D., V. Omojorla, I. Umar, and A. .. Loko. 2023. "Implementation of a 220v Ac Overload and High Voltage Monitor Alert System with Auto Shut Down." *International Journal of Engineering and Modern Technology* 8(5):32–40. doi: 10.56201/ijssmr.v8.no1.2022.pg32.40.